

# Magnetic Levitation Performance of Miniaturized Magnetically Levitated Motor with 5-DOF Active Control

Masahiro OSA\*, Toru MASUZAWA\*, Takuya SAITO\* and Eisuke TATSUMI\*\*

\*Dept. of Mechanical Engineering, Ibaraki University  
4-12-1 Nakanarusawa, Hitachi, Ibaraki 316-8511, Japan  
E-mail: masahiro.osa.630@vc.ibaraki.ac.jp

\*\*Dept. of Artificial Organs, National Cerebral and Cardiovascular Center Research Institute  
5-7-1 Fujishiro-dai, Suita, Osaka 565-8565, Japan

## Abstract

Mechanical circulatory support (MCS) therapy plays a significant role in an alternative therapy of heart transplants for pediatric heart disease patients. However, technical difficulties, such as high durability, better blood compatibility and miniature device size, prevent the pediatric MCS device development. In this study, a double stator axial gap maglev motor for pediatric MCS device has been developed. The maglev motor has two identical motor stators, and a levitated rotor impeller which is aligned between the stators. The levitated rotor impeller is fully suspended with 5-degrees of freedom (5-DOF) active control. A miniaturized maglev motor is designed and developed based on FEM magnetic field analysis for use in implantable ventricular assist devices (VADs). The developed maglev motor has an outer diameter of 22 mm and a length of 33 mm. This paper is an initial report on the magnetic levitation and rotation performance of the miniaturized maglev motor. The levitated rotor impeller is magnetically levitated and rotated with the 5-DOF active control. The oscillation amplitudes ( $x$ ,  $y$  and  $z$ ) and inclination angles ( $\theta_x$  and  $\theta_y$ ) of the levitated rotor impeller are then evaluated in both air and water. The developed maglev motor achieves non-contact rotation up to 1600 rpm in air and 4500 rpm in water, respectively. The oscillation amplitudes and inclination angles are sufficiently suppressed in water due to fluid damping. The developed maglev motor indicates potential to achieve the practical use of maglev rotatory pediatric VAD.

**Keywords** : Maglev motor, Double stator, 5-DOF active control, Ventricular assist device, Pediatric

## 1. Introduction

Severe heart disease treatment using mechanical circulatory devices have been the alternative therapy of heart transplants, due to the shortage of donor hearts. Continuous flow ventricular assist devices (VADs) which have a rotating impeller in the pump cavity accelerated downsized VADs development and contributed to the successful use of mechanical circulatory devices in adult heart failure patients. Currently, there have been increasing research interest in VADs for pediatric patients under ten years of age (Takatani, et al, 2005). However, few devices are undergoing development in the world, due to difficulties in completing design requirements: high mechanical durability, better blood compatibility, miniature device size and wide operating speed range. In 2008, a National Heart, Lung and Blood Institute issued Pumps for Kids, Infants, and Neonates (PUMPKIN) program to provide support to pediatric mechanical circulatory support devices development (Baldwin, et al, 2006, Noh, et al, 2005). Currently, a continuous flow axial flow pediatric VAD which is named Jarvik2000 is undergoing development in U.S (Gibber, et al, 2010). The Jarvik2000 device is successfully downsized up to 14 cc by employing a mechanical pivot bearing that is soaking in blood. However, the mechanical bearings of circulatory support devices still have several problems, such as low mechanical durability due to mechanical friction, blood clotting and blood cell distraction caused by heat generation and high shear stress at mechanically contacting region. In contrast, due to removing the need for contact bearing, magnetically levitated rotary VADs have significant advantages such as long life expectancy, low thrombosis, less hemolysis and high-speed operation compare to conventional blood pumps with mechanical bearings and seals

contacting with the blood (Hoshi, et al, 2006, Timms, et al, 2011, Yumoto, et al, 2009). In this study, a tiny double-stator axial gap type magnetically levitated motor that can control 5 degrees of freedom (5-DOF) of rotor impeller postures have been developed for use in pediatric continuous flow rotary VAD. Magnetic levitation performance of the developed maglev motor with newly developed 5-DOF control concept was investigated.

## 2. Materials and Methods

### 2.1 Structure and control principle of 5-DOF controlled self-bearing motor

The proposed 5-DOF controlled magnetically levitated motor is an axial gap type permanent magnet synchronous motor. The motor has a top stator, a bottom stator and a levitated rotor as shown in Fig. 1. The levitated rotor is axially sandwiched by the stators that have a completely identical structure. A double stator mechanism enhances a rotating torque production and also realizes the 5-DOF active control of levitated rotor postures. An axial position ( $z$ ) and rotating speed ( $\omega_z$ ) of the levitated rotor are controlled by using a vector control algorithm which can generate axial suspension force and rotating torque with a single rotating magnetic field (Asama, et al, 2013; Nguyen, et al, 2011; Osa, et al, 2012; Ueno, et al, 2000). The axial position of levitated rotor is actively regulated by field strengthening and field weakening as shown in Fig. 2. A rotating control flux density based on  $P \pm 2$  pole algorithm produces a restoring torque and a radial suspension force simultaneously (Osa, et al, 2012). In this theory, two rotating magnetic fields are assumed to be distributed in the air gap. One is a P pole magnetic field produced by the permanent magnet of the levitated rotor. The other is P plus or minus 2 pole magnetic field produced by the control windings. The restoring torque and the radial suspension force can be produced independently with double stator mechanism. As shown in Fig. 3, an inclination angle around y-axis and a radial position in x direction of levitated rotor can be controlled actively. Both stators produce restoring torque in the same direction; the radial forces produced by stators cancel each other, and the restoring torque produced. In contrast, the restoring torque produced by top stator and bottom stator is regulated in opposite direction, and then the radial suspension force can be generated. In a similar manner, the inclination control around x-axis and the radial position control in y direction are available. Consequently, the inclination angles ( $\theta_x, \theta_y$ ) and the radial positions ( $x, y$ ) of levitated rotor can be controlled by regulating the magnitude and the direction of restoring torque and radial suspension force by regulating excitation currents supplied to the top stator and the bottom stator.

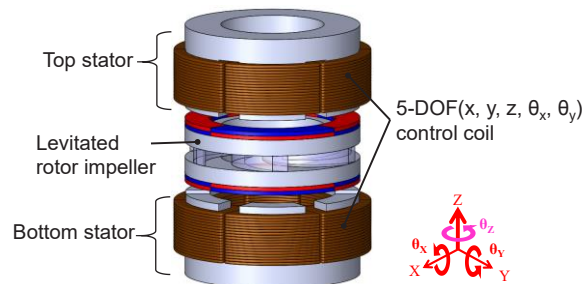


Fig. 1 Structure of proposed 5-DOF controlled maglev motor.

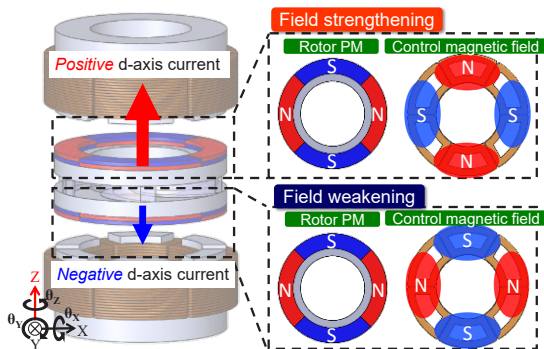


Fig. 2 Axial suspension force production with field strengthening control and field weakening

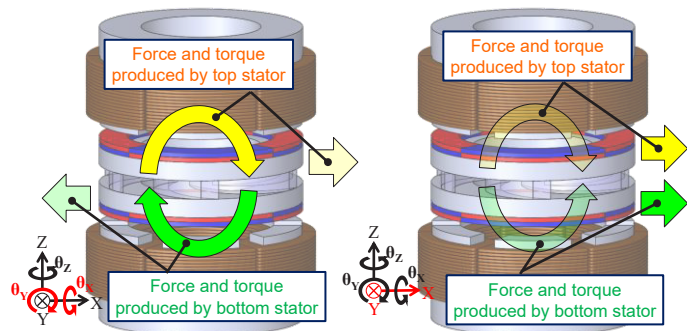


Fig. 3 Independent control of restoring torque and radial suspension force with  $P \pm 2$  pole algorithm.

## 2.2 Miniaturized motor design with 3D FEM magnetic field analysis

### 2.2.1 Identification of required motor torque and suspension force characteristics

The pediatric VAD requires a maximum output power of 0.5 W to produce flow rates of 0.5 ~ 1.5 L/min against a head pressure of 100 mmHg at rotating speeds of 3500 ~ 4500 rpm. Assuming a hydraulic efficiency of 20 % in pediatric circulation support, the maglev motor has to generate an output power up to 2.5 W. A required torque of the maglev motor is calculated to be 5.3 mNm at the rated rotating speed of 5000 rpm. With a double stator mechanism, torque requirement for each stator is 2.7 mNm. In addition, suspension force characteristics of the maglev motor should be identified to achieve stable levitation and better vibration suppression performance. The motor must balance the forces that are produced by the top motor and the bottom motor over the full range of rotor displacements. The required attractive force for each motor stator is determined to be 1.0 N per unit ampere that indicates ten times greater than the mass of the rotor.

### 2.2.2 Double stator type magnetically levitated motor design

The 3-D finite element method (FEM) analysis was carried out to determine motor geometries, such as a stator diameter, cross sectional area of stator tooth and volume of rotor permanent magnets. 3-D models of the motor components shown in Fig. 4 was simulated in ANSYS. The designed motor has six stator slots and four pole permanent magnets. An outer diameter of the motor is 22 mm. An air gap length of the motor is determined to be 1.5 mm that include the pump casing and blood gap. The number of turns in stator windings is 66. A magnetic suspension force and a rotating torque characteristics were computed considering the distribution of magnetic flux density, leakage flux and the magnetic saturation of the motor core. The magnetic flux is most concentrated in the stator tooth at the airgap length of 1.5 mm and the rated excitation current of 2 A. The magnetic field distribution in this condition is shown in Fig. 5, and the result indicates that there is no magnetically saturated parts. Fig. 6 and Fig. 7 show an estimated attractive force and rotating torque with the excitation current of 0 ~ 2 A. The calculated force and torque are sufficiently greater than the identified target performances.

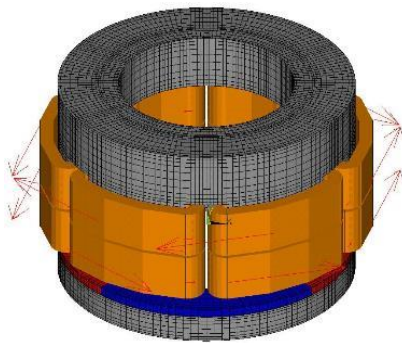


Fig. 4 Assembled 3-D model simulated in ANSYS.

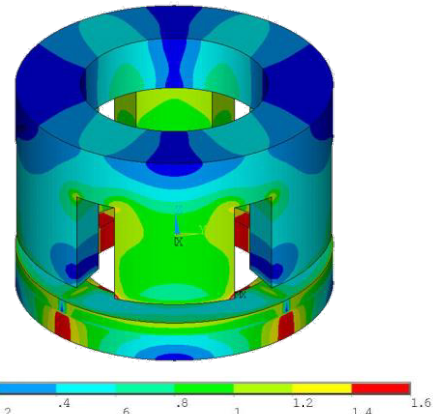


Fig. 5 Contour result of magnetic flux density.

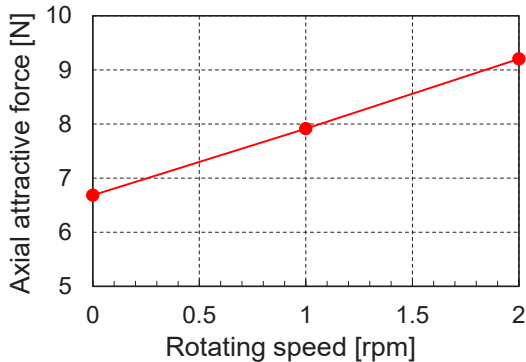


Fig. 6 Axial attractive force characteristics.

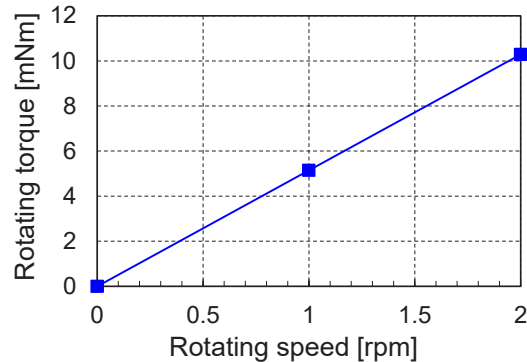


Fig. 7 Rotating torque characteristics.

### 2.3 Fabrication of miniaturized 5-DOF controlled maglev motor

A 5-DOF controlled maglev motor was developed referring to a finally determined motor geometries. The schematic of the developed motor is shown in Fig. 8. Specifications of the motor geometries and rotor permanent magnets are shown in Table 1. The developed motor has an outer diameter of 22 mm, a height of 33 mm and a magnetic air-gap length of 1.5 mm. The weight of the levitated rotor is 11 g. The thickness of the rotor permanent magnets is 1.0 mm. The motor stator and the rotor back iron are made of soft magnetic iron (SUY-1). The permanent magnets are made of Nd-Fe-B which has a coercivity of 907 kA/m and a residual flux density of 1.36 T. The number of turns in the concentrated windings wound on each stator tooth is 66. Concentrated copper windings are independently wound on each stator tooth. The diameter of isolated copper wire is 0.3 mm. Resistance and inductance of each coil with different exciting frequency of 0 ~ 1 kHz are 0.76 ~ 0.90  $\Omega$  and 147  $\mu$ H, respectively.

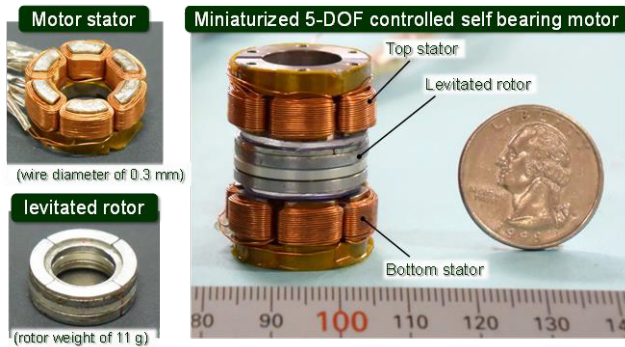


Fig. 8 Developed 5-DOF controlled maglev motor.

Table 1 Specifications of the maglev motor.

|   |     |
|---|-----|
| Inner diameter of the rotor and stator [mm]         | 16  |
| Outer diameter of the rotor and stator [mm]         | 22  |
| Total height of the maglev motor [mm]               | 33  |
| Total volume of the maglev motor [cm <sup>3</sup> ] | 13  |
| Height of stator teeth [mm]                         | 7.3 |
| Thickness of rotor back iron [mm]                   | 2   |
| Thickness of permanent magnets [mm]                 | 1   |
| Pole pair number of permanent magnet [-]            | 4   |

### 2.4 Magnetic levitation and rotation control system with digital PID controller

5-DOF of the levitated rotor postures and rotating speed of the rotor are actively regulated with digital PID controllers that are implemented on a micro-processor board DS1104 (dSPACE GmbH, Paderborn Germany) with MATLAB/Simlink. A schematic of a 5-DOF control system is shown in Fig. 9. Power amplifier (PA12A, Apex Microtechnology Corporation) supplies the calculated control current to control windings of both stators. Sampling and control frequency is 10 kHz. Three eddy current sensors (PU-03A, Applied Electronics Corporation) are set onto inner side of stator tooth to measure axial position and inclination angles around x and y axes of the levitated rotor. Other two eddy current sensors are set on x-axis and y-axis to measure radial positions of the levitated rotor. Three Hall Effect sensors (Asahi KASEI Corporation) are set at stator slots to detect the rotating angles of the levitated rotor with a sensitivity of 30 degrees electrical angle. The rotating speed at increments of 180 degrees (mechanical angle) is determined by the rotating angle divided by the time it takes to rotate the rotor 90 degrees.

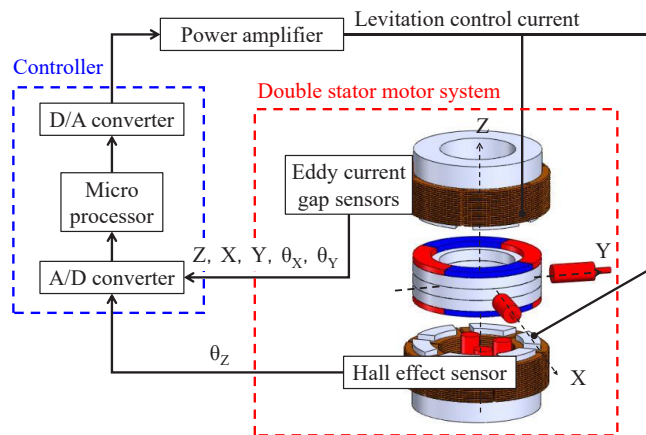


Fig. 9 Schematic of 5-DOF control and rotation control system.

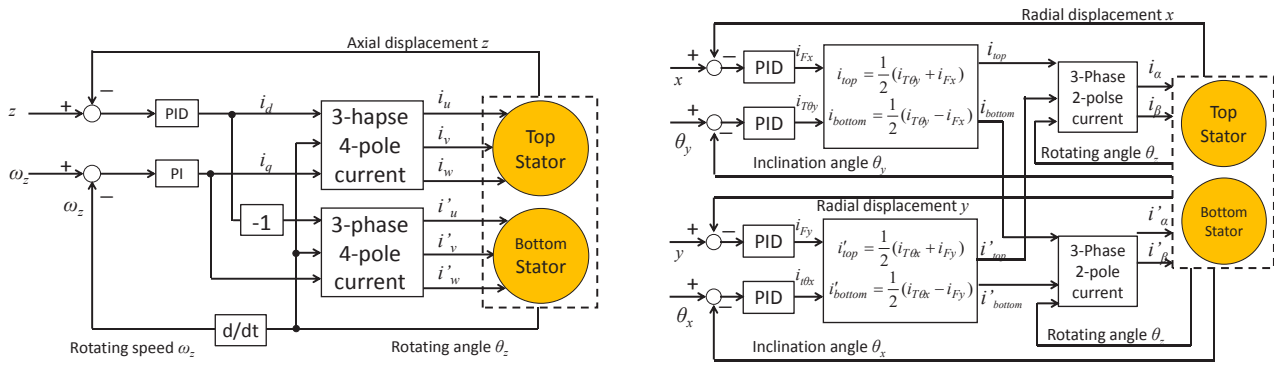


Fig. 10 Diagram of PID controller: (a) axial position and rotation control system, (b) radial position and inclination control system.

A block diagram for axial position and rotation control is shown in Fig. 10. The axial position of the levitated rotor is stabilized by regulating d-axis current  $i_d$  with a PID feedback loop shown in Fig. 10 (a). Positive and negative d-axis currents which are for field strengthening and field weakening generate an unbalanced magnetic attractive force in rotor axial direction. The rotating speed is controlled by regulating q-axis current  $i_q$  with the PI feedback loop. The calculated q-axis current for both stator windings are equal to  $i_q$ . The d-axis current  $i_d$  and the q-axis current  $i_q$  are transformed into three-phase current  $i_u, i_v$  and  $i_w$ . Then these currents are supplied to control windings of both stators to generate an four pole rotating magnetic field. A diagram for the inclination angle and radial position control is shown in Fig. 10 (b). The inclination angle  $\theta_y$  control corresponds to the radial position  $x$  control, and the inclination angle  $\theta_x$  control corresponds to the radial position  $y$  control. The required excitation current for generating the restoring torque and the radial suspension force, is calculated using the PID feedback loop. These excitation currents are supplied to the inclination angle and radial position control windings to generate two pole rotating magnetic field which has common rotating angular frequency of the magnetic field produced by the rotor permanent magnets.

## 2.5 Magnetic suspension performance evaluation

Magnetic levitation and rotation tests were carried out to verify non-contact rotation with the developed 5-DOF controlled maglev motor. The maglev motor and a magnetic levitation test rig were assembled as shown in Fig. 11. The movable ranges of the rotor in the axial and radial direction are restricted to  $\pm 0.3$  mm and  $\pm 0.5$  mm, respectively. Control gains of each digital PID controllers shown in Table 2 were determined based on experimentally measured suspension force and torque characteristics. The P gain and I gain of a rotating speed PI controller were 0.00075 A/rpm and 0.007 A/(sec · rpm) respectively. The rotor was levitated with 5-DOF control and a rotating speed of the magnetically levitated rotor was increased. In practical use of the maglev motor, the levitated rotor is in a fluid medium, so that a viscosity of the fluid affects damping characteristics in rotor suspension. Then, experiments were carried out once in air, and once in a water which is chosen due to simplicity of use. Oscillation amplitude in the axial and radial direction, and maximum inclination angles around x and y axes were measured. The maximum oscillation amplitude was defined as half of the peak-to-peak value of rotor vibration.

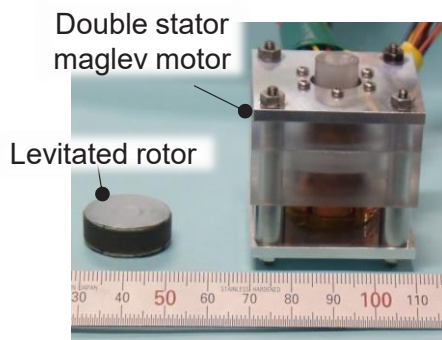


Fig. 11 Magnetic levitation and rotation test rig

Table 2 Specifications of the maglev motor.

| Gain              | P                   | I                  | D                      |
|-------------------|---------------------|--------------------|------------------------|
| Radial position   | 1.5<br>[A/mm]       | 12<br>[A/mm]       | 2.2<br>[A/deg]         |
| Axial position    | 0<br>[A/sec mm]     | 0.07<br>[A/sec mm] | 0.07<br>[A/sec deg]    |
| Inclination angle | 0.002<br>[A sec/mm] | 0.08<br>[A sec/mm] | 0.00275<br>[A sec/deg] |



### 3. Experimental results

#### 3.1 Magnetic levitation performance evaluation

The rotor was successfully levitated and rotated in both air and water. The maximum rotating speeds with no mechanical contact were 1600 rpm in air and 4500 rpm in water, respectively. The oscillation amplitude of the axial vibration of the rotor is shown in Fig. 12. The maximum oscillation amplitude was 0.1 mm at 1400 rpm in air and 0.05 mm at 4000 rpm in water. The axial oscillation increased drastically when the rotating speed was 1800 rpm. The axial vibration was significantly reduced at every rotating speeds when water was used. Fig. 13 shows the radial oscillation amplitude of the radial vibration of the rotor. The radial oscillation amplitude increased as the rotating speed increased in air. The levitated rotor touched the casing radially at 1800 rpm. In contrast, the oscillation amplitudes were less than 0.3 mm at all rotating speeds in water. Fig. 14 shows the maximum inclination angles around radial axes of the levitated rotor. The inclinations of the levitated impeller were greatly increased at the rotating speed of 1800 rpm in air. It can be seen that the levitated impeller was touching down constantly. When operating in water and at the rotating speed range of 1000 rpm to 4500 rpm, the inclinations were maintained around 1.2 degrees.

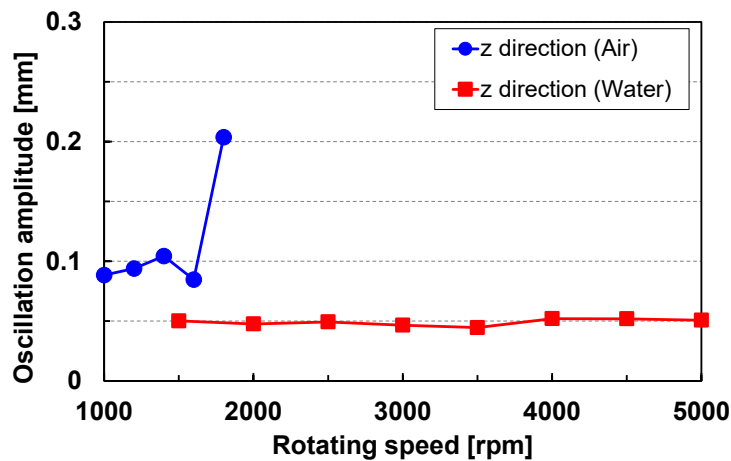


Fig. 12 Oscillation amplitude in axial direction of the levitated rotor

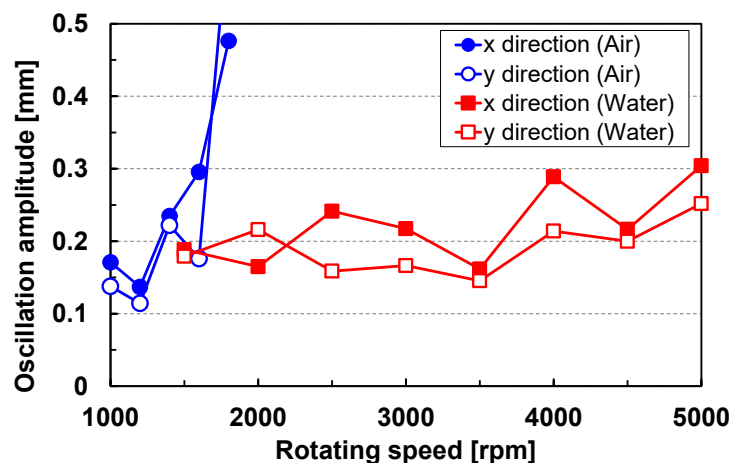


Fig. 13 Oscillation amplitude in radial directions of the levitated rotor.

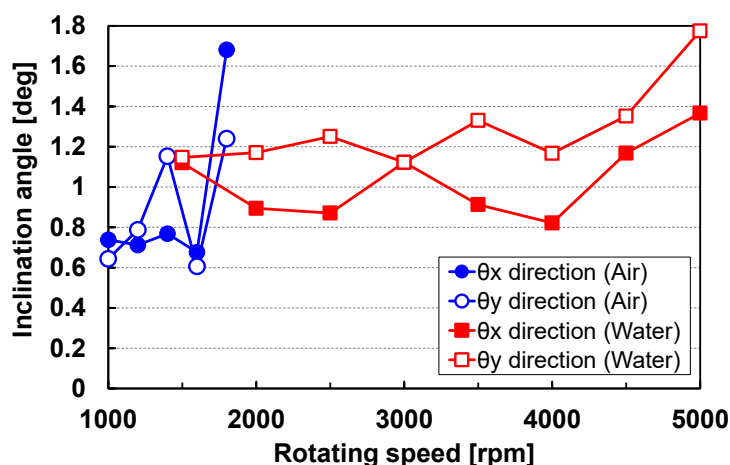


Fig. 14 Maximum inclination angle round radial axes of the levitated rotor.

#### 4. Discussion

Magnetic suspension system is a viable suspension technique to enhance mechanical durability and blood compatibility of the rotary VAD. The developed 5-DOF controlled maglev motor, which is miniaturized up to 22 mm in diameter and 33 mm in height, will contribute to the development of next generation pediatric VADs which can be applied to heart disease patients under ten years of age.

The 5-DOF of levitated rotor postures were significantly stabilized with water viscous damping. In particular, the oscillation amplitude in the axial direction was sufficiently decreased by half amplitude that is demonstrated by the experiment in air. The mechanical contact was prevented by water damping over the VAD operating range of 3500 ~ 4500 rpm, however, the inclination angles increased according to the increase in rotating speed. The levitated rotor then touched down a number of times at more than the rotating speed of 4500 rpm. The inclination controllability is restricted by the rated current of 2 A which is desirable in order to limit generating heat of the VAD system. From the results, the inclination control capacity should be enhanced to achieve further stable levitation by optimizing the motor geometry and the PID control system. In practical VAD operation, further high speed rotation with no contact will be achieved utilizing a greater vibration suppression due to blood viscosity that is three times higher than that of water.

In the future, total optimization of the magnetic system, such as motor geometric design, the material of magnetic core and the rotor permanent magnet, gains of PID controller, will be conducted to combine with a miniaturized centrifugal blood pump. Then, dynamic characteristics of the developed 5-DOF controlled maglev motor will be evaluated in VAD pump operation.

#### 5. Conclusion

The axial gap type double-stator maglev motor which can actively control 5-DOF of rotor postures was developed for use in magnetically levitated rotary pediatric VAD. The significant effect of viscous damping on the performance of the magnetic system was demonstrated. The developed maglev motor indicated sufficient magnetic suspension and rotation performance to maintain stable non-contact operation at speeds required for the pediatric VAD circulatory support. The results verified a potential of the next generation implantable pediatric VAD system.

#### References

Takatani S., Hoshi H., Tajima K., Ohuchi K., Nakamura M., Shinshi T. and Yoshikawa M., Feasibility of a Miniature Centrifugal Rotary Blood Pump for Low-Flow Circulation in Children and Infants, *ASAIO Journal*, Vol. 51, No. 5,

(2005), pp. 557–562.

- Baldwin J. T., Borovets H. S., Duncan B. W., Gartner M. J., Jarvik R. K., Weiss W. J. and Hoke T. R., The National Heart, Lung, and Blood Institute Pediatric Circulatory Support, *Circulation*, Vol. 113, (2006), PP. 147–155.
- Noh, M.D., Antaki, J. F. and Gardiner M. R., Magnetic Levitation Design for the PediaFlow Ventricular Assist Device, *Proc. 2005 IEEE/ASME International Conference on Advanced Intelligent Mechatronics*, (2005), pp. 1077–1082.
- Gibber M., Wu Z. J., Chang W., Bianchi G., Hu J., Garcia J., Jarvik R. and Griffith B. P., In Vivo Experience of the Child-Size Pediatric Jarvik 2000 Heart: Update, *ASAIO Journal*, Vol. 56, No. 4, (2010), 369–376.
- Farrar D. J., Bourque K., Dague. C. P., Cotter C. J. and Poirier V. L., Design Features, Developmental Status, and Experimental Results With the Heartmate III Centrifugal Left Ventricular Assist System with a Magnetically Levitated Rotor, *ASAIO Journal*, Vol. 53, No. 3, (2007), pp. 310–315.
- Hoshi H., Shinshi T. and Takatani S., Third-generation Blood Pumps With Mechanical Noncontact Magnetic Bearings, *Artificial Organs*, Vol. 30, No. 5, (2006), pp. 324–338.
- Timms D. L., Kurita N., Greatrex N. and Masuzawa T., BiVACOR A Magnetically Levitated Biventricular Artificial Heart, *Proc. of MAGDA conference in Pacific Asia*, (2011), pp.482–487.
- Yumoto A., Shinshi T., Zhang X., Tachikawa H. and Shimokohbe A., A One-DOF Controlled Magnetic Bearing for Compact Centrifugal Blood Pumps, *Motion and Vibration Control*, Springer Science+Business Media B.V. , (2009), pp. 357–366.
- Asama J., Hamasaki Y., Oiwa T. and Chiba A., Proposal and Analysis of a Novel Single-Drive Bearingless Motor, *IEEE Transactions on Industrial Electronics*, Vol. 60, No. 1, (2013), pp. 129–138.
- Nguyen Q. D., Ueno S., Analysis and Control of Nonsalient Permanent Magnet Axial Gap Self-Bearing Motor, *IEEE Transactions on Industrial Electronics*, Vol. 58, No. 7, (2011), pp. 2644–2652.
- Osa M., Masuzawa T. and Tatsumi E., Miniaturized axial gap maglev motor with vector control for pediatric artificial heart, *Journal of JSAEM*, Vol. 20, No. 2, (2012), pp. 397–403.
- Ueno S., Okada Y., Characteristics and Control of a Bidirectional Axial Gap Combined Motor-Bearing, *IEEE/ASME Transactions on Mechatronics*, Vol. 5, No. 3, (2000), pp. 310–318.
- Osa M., Masuzawa T. and Tatsumi E., 5-DOF control double stator motor for paediatric ventricular assist device, *Proceedings of ISMB13*, (2012), paper41.